Effects of Geomagnetic Storms in the Low-Latitude Ionosphere

D. V. Blagoveshchensky*

St. Petersburg State University of Aerospace Instrumentation,
St. Petersburg, 190000 Russia
*e-mail: donatbl@mail.ru

Abstract—A wide range of changes in parameters of the low-latitude ionosphere has been revealed during the periods of three intense geomagnetic storms that occurred in different seasons of 2015. Ionospheric parameters, according to the data from ionosondes (ionograms), include critical frequencies $foF2$, foE, and $foEs$; the degree of diffuseness of signals; the presence of lateral reflections; the multihop pattern of vertical-incidence ionospheric sounding (VIS); the effect of blocking signal reflections from the $F2$ layer by the Es layer; and the presence of M-type modes. The analysis was based on the data from ionosondes at low-latitude stations in Athens, Greece, and Nicosia, Cyprus. The following results were obtained. The spring storm was characterized by the presence of lateral reflections, greater diffuseness in the $F2$ layer, and an increased number of reflections during VIS during daytime hours compared to nighttime hours. The summer storm was characterized by very frequent appearance of sporadic Es layers, the occurrence of M-type reflections, and the effect of blocking. The specific analysis of the winter storm shows that the thick Es layer stretched along the Earth's surface over a distance of no less than 800 km and had a lifetime of about 7 h.

INTRODUCTION

Nonstationary processes in the interplanetary medium and Earth's magnetosphere are known to be triggered by active regions on the Sun, e.g., flares and coronal holes. The energy of solar disturbances is released as electromagnetic and corpuscular radiations, blast waves, and mass ejections. The onset of interaction between the blast wave and the magnetosphere determines the moment of onset of its disturbance; there is a storm sudden commencement (SSC) appearing as a hop of the H-component of the geomagnetic field due to the field of currents flowing along the surface of the magnetosphere. Magnetic storms are characterized by extremely high disturbance of the magnetosphere [4, 8, 9]. An ionospheric storm is a global disturbance of total electron content (TEC), electron concentration in the F-region maximum, and the peak height during a geomagnetic storm as a result of different dynamic and chemical processes: energetic particle precipitation, changes in electric fields and current systems, moving atmospheric disturbances, thermospheric circulation, compositional changes, etc. At present, the statistical pattern of storms is already known to a certain extent. The long-term decreases in electron concentration in the $F2$ layer and in the total electron content in the main phase of the storm, especially in the middle latitudes, can be considered a main indicator of a storm in the $F2$ layer of the ionosphere [3, 5]. This negative phase is often preceded by a positive one, which can appear in the low latitudes within the main phase and in the middle latitudes in winter. This classical pattern of ionospheric storm is based on the statistical analysis in reviews [1, 4] and has been confirmed by many observations, e.g., [7]. Work [6] presents an analysis of ionospheric effects of geomagnetic storms in the European region, where the critical frequency of the $F2$ layer is much higher or lower than the median level, depending on the season and the time of onset of the disturbance, and a model has been developed to predict the behavior of ionospheric parameters during the storm. The global response to geomagnetic storms, proceeding from data from the ionosonde network, has been investigated in work [10]. Low latitude auroras were observed over very large regions in the northern and southern hemispheres. A long-term decrease of ionization in the middle latitudes is the most marked effect of a storm. Although ionospheric storm has been an object of research for decades, its effects have not been fully explained so far. The state of the ionosphere during the storm depends on a great number of variables, such as local time, geomagnetic latitude, season, solar activity, time of storm onset, time of storm (the time that has passed since the onset of the storm), storm intensity, and prestorm activity (large storms are rarely isolated). In addition, the physical processes controlling the global ionosphere and the atmosphere is complicated by the fact that geomagnetic disturbances are insufficiently predictable. Data analysis shows that the ionosphere is most strongly affected by magnetic

storms in the high latitudes, which affects variations in its parameters. Much less attention has been paid to low latitudes (except for the effect of decrease in $NmF2$ and TEC).

The main goal of this work was to find out how ionospheric parameters in the low latitudes vary during rather intense geomagnetic storms. Ionospheric parameters obtained by the ionosonde data include $foF2$, foE, and $foEs$; the degree of diffuseness of signals; the presence of lateral reflections; the multihop pattern of vertical-incidence ionospheric sounding (VIS); the effect of blocking; and the presence of M-type modes. The data used for analysis were obtained by vertical incidence sounding at low-latitude stations in Athens (38.00° N, 23.50° E) and Nicosia (35.03° N, 33.16° E) from the website http://ulcar.uml.edu/didbase. The ionograms from this website were analyzed every 2 h on a 24-h basis, i.e., 12 ionograms per day.

CHARACTERISTICS OF GEOMAGNETIC STORMS

All in all, three geomagnetic storms were chosen for the analysis: one in spring, the second in summer, and the third in winter of 2015. Here, it will be advisable to identify seasonal differences, because the ionosphere has specific characteristics for each season. Geostorm characteristics are given in Table 1. From the table, it follows that the storm of March 17−20, 2015, was the most intense. The two other storms were less intense, but also rather strong [8]. The first and third storms have almost identical onsets of the main phase and identical onsets of the restoration phase, while the second storm differs in these parameters from the first and third ones. The durations of all three storms were also different.

Magnetic Storm of March 17−20, 2015

First, let us consider the three almost quiet days before the storm of March 17−20 at the Athens station. Here, $\Sigma Kp = 11-$ for March 14, $\Sigma Kp = 14-$ for March 15, and $\Sigma Kp = 19-$ for March 16. The onset of disturbance on March 17 is characterized by $\Sigma Kp = 48$. Thus, the interval of March 14−16 is of interest. Here, $foF2$ varies slightly from day to day. The values show an obvious daily dependence: an increase from midnight ($foF2 = 4.5$ MHz on average) to 10.00 am ($foF2\text{max} = 11.5$ MHz on the average) at 10.00 am. There is then again a decline by the end of the day to the initial value of $foF2 = 4.7$ MHz. The foE values are recorded infrequently: two to three values before 10.00 am. The $foEs$ values, on the contrary, are recorded after 10.00 am; again, two to three values. In addition, there is a tendency for the number of hops in vertical sounding to decrease from midnight (three or four) to the daytime hours (one) and to increase again by the end of the day (three to four). This is most likely associated with the disappearance of the D layer at

Table 1. Parameters of geomagnetic storms used for analysis

Onset of main phase by Dst	Dst_{min}, nT	Onset of restoration	T_e, end of storm
8.00 am March 17	−223	10.00 pm March 17	5.00 pm March 21
1.00 pm June 22	−204	5.00 am June 23	5.00 am June 25
6.00 am December 20	−155	10.00 pm December 20	11.00 pm December 23

night and the decrease in absorption. Parameters such as diffuseness, the presence of lateral reflections, and the blocking effect are absent. Let us now consider the disturbed days of March 17−20. It would be advisable to compare the data on the disturbed days with the data on the quiet days of March 14−16. The first disturbed day, March 17, shows an absence of any significant changes in ionospheric parameters. Most likely, it is exhibiting some inertness here. For example, the $foF2$ values for March 17 were similar to the values for March 16. Sporadic Es were not observed at all. The foE values were recorded three times in the morning. They corresponded to the values for March 16. The only difference between the disturbed day and the quiet day was the appearance of lateral reflections in the second half of the day (twice). In other respects, there were no differences. The disturbed day of March 18 ($\Sigma Kp = 39+$) has noticeably different parameters than does the quiet day of March 16. First of all, here there is an appreciable decline in $foF2$ values after midday (10.00 am) to the end of the day. This fact (the $foF2$ decrease during the geomagnetic storm) is generally known and confirmed here. As regards the values of $foEs$ and foE, they are recorded just as rarely as on the quiet day. Now let us consider the differences. First of all, lateral reflections were observed over the course of the disturbed day of March 18. They were most likely determined by perturbations in the ionosphere during the storm. In addition, since the morning of March 18, there had been a considerable increase in the diffuseness of the $F2$ layer. The example of lateral reflection and diffuseness in the $F2$ layer is given in Fig. 1 for March 18 at 4.00 am. This ionogram shows intense diffuseness in the ranges of 3−5 MHz and 350−550 km at the first hop. Lateral reflection is recorded at a frequency of 8 MHz and a height of 1100 km. Another peculiar feature of the day of March 18 compared to the undisturbed day is that the number of hops of reflections in vertical sounding increases to three instead of one in daytime hours. The disturbed days of March 19 and 20 are characterized by a minor decrease in the degree of disturbance (from $\Sigma Kp = 30+$ to 28). Most importantly, the $foF2$ values are much lower than the values for quiet conditions. This is typical of intense magnetic storm. Parameters $foEs$ (two cases) and foE
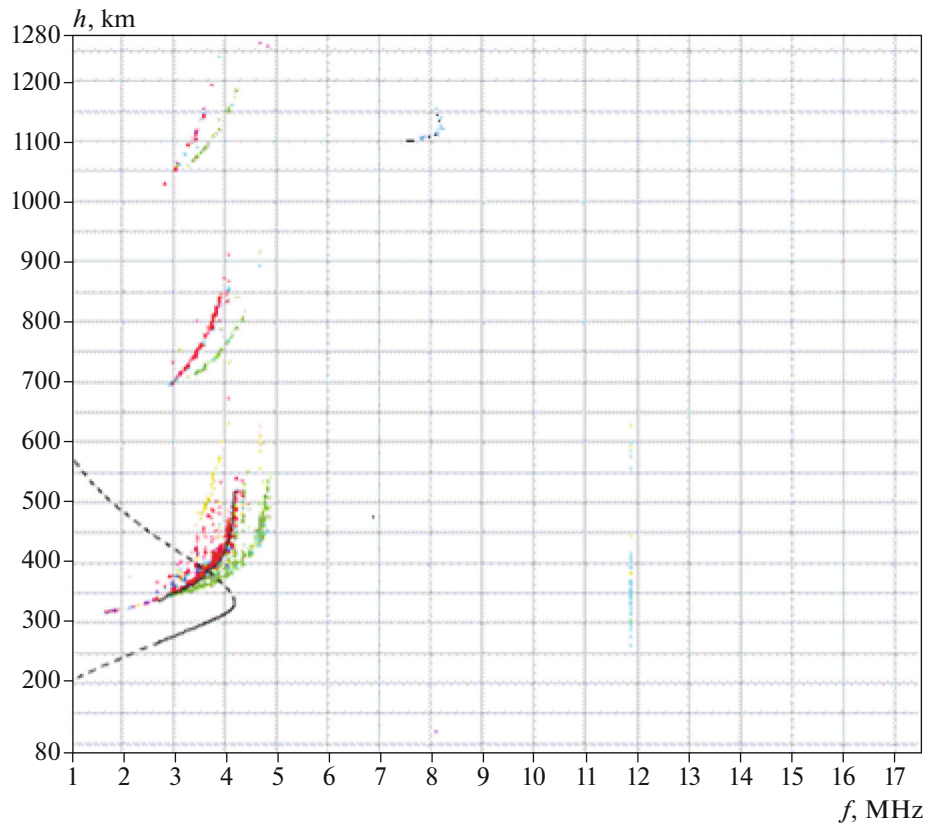
Fig. 1. A ionogram of vertical-incidence ionospheric sounding (VIS) at the Athens station showing the diffuseness in the $F2$ layer (4 MHz, 450 km) and the presence of lateral reflection (8 mHz, 1130 km).

(four cases) have values of 3−4 MHz and are concentrated around midday. There is no diffuseness on the days under consideration. The number of lateral reflections decreases with decreasing degree of disturbance. For example, there are eight of them on March 19 and only four on March 20. Finally, the number of hops in vertical sounding is similar to their number under quiet conditions: one hop around midday.

To sum up, the extraordinary effects at the maximum disturbance compared to the quiet period are as follows: the presence of lateral reflections, the increased diffuseness in the $F2$ layer, and the increased number of reflections during vertical sounding in daytime hours compared to nighttime hours. It has been confirmed that disturbance in the low latitudes is accompanied by a decrease in the $foF2$ value compared to the quiet period. Very few occurrences of sporadic Es layers is a peculiarity of a geostorm (as a season of the equinox).

Magnetic Storm of June 22−25, 2015

The three quiet days before the onset of disturbance were as follows: June 19 with $\Sigma Kp = 6-$, June 20 with $\Sigma Kp = 1+$, and June 21 with $\Sigma Kp = 12$. Ionospheric parameters on these days are insignificantly different. As has been mentioned above, the $foF2$ values demonstrate daily variations: they increase from 6 MHz at midnight to 9 MHz at midday (10.00 am) and decrease again to 6 MHz at midnight (on the average). The foE values are recorded around midday (four to seven cases with $foE = 2-3.5$ MHz). As regards the $foEs$ values, the situation here is dramatically different from that of the storm of March 17−19. There is an almost 24-h occurrence of sporadic layers—to be more exact, over 80%. At the same time, the $foEs$ values are in the range of 3−9 MHz. Diffuseness is observed both in the $F2$ layer and in the Es layer mostly in the nighttime hours. There are few reflections of signals in VIS in daytime hours (one, rarely two), but their number increases to three by night. Lateral reflections are not observed at all. Here, as before, the data on quiet days will be compared to the data on disturbed days. Let now consider the disturbed days of June 22−25. The onset of the main phase of the storm was at 1.00 pm of June 22 ($\Sigma Kp = 35+$). The Dst index reached its minimum: $Dst = -204$ nT on June 23 ($\Sigma Kp = 42-$) at 5.00 am (the maximum of disturbance). The phenomenon of blocking $F2$-reflections by sporadic Es-reflections ($foEs > foF2$) is observed within a few hours close to the minimum of the Dst index. Here, there is no increase in the $foEs$ values but a decrease in the $foF2$
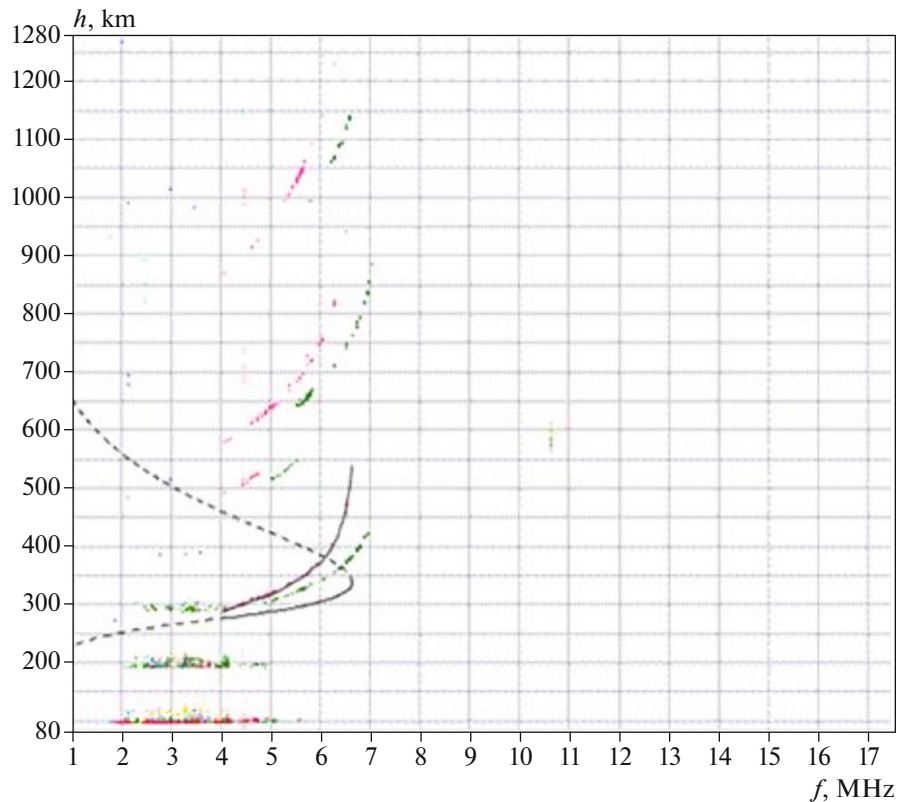
Fig. 2. VIS ionogram at the Athens station showing the multihop reflections from the *Es* layer (2−5 MHz) and the *M*-reflection (5 MHz, 520 km).

values during a strong disturbance, which results in blocking. An example of blocking on the ionogram is given in Fig. 4. There are no lateral signals for June 22 and 23. This is a difference from the previous storm of March 17−19. Characteristically, there are so-called "*M*-reflections" on June 24 ($\Sigma Kp = 23+$) according to VIS data [2]. The essence of *M*-reflection is that a beam goes upward from the Earth's surface, is reflected from the *F*2 layer and turned to the underlying *Es* layer, is reflected again from the latter and goes upward to the *F*2 layer, and then is reflected from it and descends to the Earth. Such behavior is most likely to be explained by the presence of rather thick sporadic layers. The example of *M*-reflection is given on the ionogram for June 24 at 8.00 pm in Fig. 2. Here, *M*-reflection occurs within a range of 4.5−5.5 MHz and at a height of 520 km between the first and second hops. It is noteworthy that, in contrast to the previous storm of March 17−20, the storm under consideration is accompanied by very frequent occurrence of sporadic *Es* layers with $foEs = 2$−9 MHz. Thus, these layers appear on the disturbed days (June 24 and 25) on a 24-h basis. Due to their intensity, they are characterized by two to four reflections from the ionosphere at night and in the evening. Examples of intense sporadic layer *Es* with a multihop pattern are given in Fig. 2, with four hops in the range of 2−5 MHz, and by anal-

ogy in Fig. 4. The latter shows that the sporadic layer completely blocks the *F*2 layer. As regards the *E* layer, the *foE* values are recorded equally often on the quiet and disturbed days.

To sum up, a very frequent occurrence of sporadic *Es* layers, *M*-type reflections, and the effect of blocking are specific characteristics of this storm. That there are no lateral reflections during the storm is an extraordinary fact. Naturally, in most cases, the *foF*2 values during this disturbance are lower than in the quiet period. Finally, let us note that ionospheric parameters recorded on the VIS ionograms for this storm differ from the parameters of the preceding storm.

Magnetic Storm of December 20−22, 2015

Let us begin with considering the three quiet days before the onset of the magnetic storm. These are December 17 with $\Sigma Kp = 11$, December 18 with $\Sigma Kp = 9$, and December 19 with $\Sigma Kp = 15-$. All these days have approximately the same ionospheric parameters. For example, the *foF*2 values are about 3.2 MHz (on the average) at midnight, then increase to $foF2 = 7.3$ MHz at the local midday at 10.00 am and decrease again to $foF2 = 3.2$ MHz at 22.00 pm. The *foEs* parameter is recorded several times around midday and lies within $foEs = 2.5$−4.0 MHz. Accordingly, *foE* is also recorded
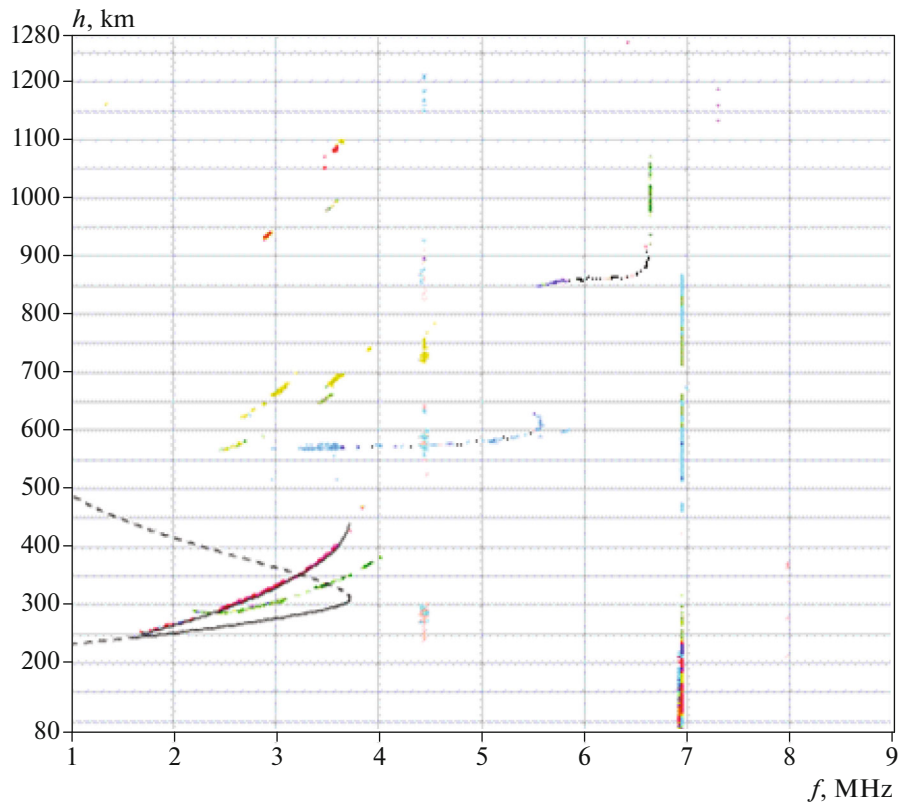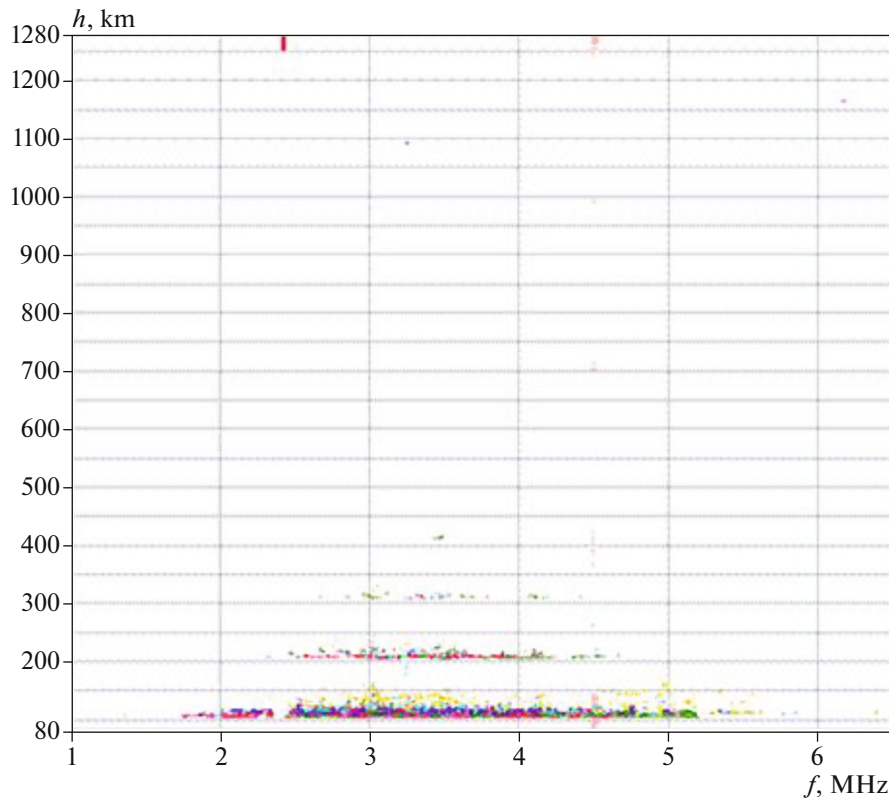
Fig. 3. VIS ionogram at the Athens station showing lateral reflections: first (6.6 MHz, 870 km) and second (5.5 MHz, 600 km).

around midday two or three times with values of about 2.3−2.9 MHz. The number of hops is two to three in the morning and in the evening and one around midday. Diffuseness, lateral signals, M-modes and blocking are absent on these three days. The first strongly disturbed day for this storm is December 20 with $\Sigma Kp = 45-$. Now, it is different from the quiet days. There is an increase in the number of occurrences of sporadic layers (four instead of two or three) and the $foEs$ values. There is also diffuseness in these layers (three cases). Lateral reflections are observed. The number of hops in the daytime hours increases to two or three instead of one. However, the foE parameter remains the same as on the quiet days. The M-modes and the blocking effect are not observed either. The next disturbed day of this storm, December 21 ($\Sigma Kp = 31$), corresponds to the minimum of the Dst-index. This day is characterized by substantial changes in the ionosphere compared to the quiet days. First of all, there is an increased number of occurrences of sporadic Es layers with higher values of $foEs = 3.0-4.5$ MHz, although disturbance had no effect on the foE values. The number of hops around midday also increases to three instead of one. There are some cases of diffuseness both in the F layer and in the Es layer. The characteristic feature is the presence of lateral reflections, M-modes (see Fig. 2), and blocking effect. The example of lateral reflections is given in Fig. 3 for

December 21 at midnight. The ionogram shows the first lateral signal in the frequency range of 5.5−6.7 MHz and at heights of 850−900 km. The second lateral signal has coordinates of 3.2−5.5 MHz and 570−630 km, with the inflection point of the curve at 5.5 MHz at a height of 600 km. It was of interest to compare the presence of lateral reflections at the same time for the stations in Athens and Nicosia, the distance between them being approximately 800 km. It has been shown that, at the Nicosia station, there is one lateral signal with an inflection point at a frequency of 5.5 MHz and at a height of 500 km. Consequently, it is highly likely that the ionospheric region generating the lateral signal is common for Athens and Nicosia, because the lateral signal is present simultaneously on the ionograms of Athens and Nicosia. Figure 4 shows an example of blocking. Here, the $F2$ layer is blocked by the underlying Es layer with a high value of $foEs = 4.63$ MHz. This layer is so thick and diffuse that it generates a multihop pattern in the form of four reflections at heights of 102.5 (first), 205 (second), 307.5 (third) and 410 km (fourth). Since the layer under consideration is rather intense, here it is also possible to compare the ionograms of Athens and Nicosia. The ionogram for Nicosia is shown in Fig. 5. Here, there is a diffuse sporadic Es layer with $foEs = 2.63$ MHz, which is found at the height of 101.3 km. The first hop from the Es layer occurs at the height of 101.3 km, and the second one

Fig. 4. VIS ionogram at the Athens station showing the multihop pattern of signal reflection from the *Es* layer (2–5.5 MHz) and the effect of blocking the *F*2 layer by the *Es* layer.
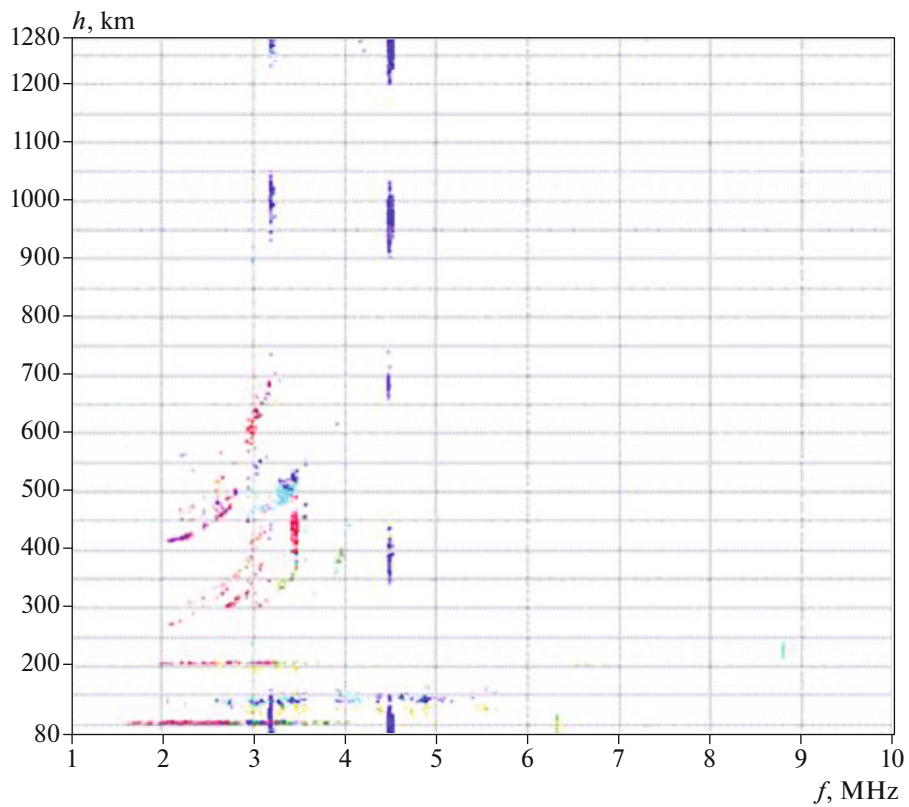
Fig. 5. VIS ionogram at the Nicosia station showing the intense *Es* layer (2–4 MHz) and diffuseness in the *F*2 layer (2–3.5 MHz, 300–700 km).

occurs at the height of 202.6 km. These data suggest that the *Es* layer in this case stretches along the Earth's surface to a distance of no less than 800 km. In addition, the lifetime of this layer, according to the data from the Athens ionosonde, lies within a range of 9.00 pm−3.45 am = 6 h 45 min. Here, the maximum $foEs = 6.4$ MHz is observed at 9.30 pm for December 21. Then, Fig. 5 shows strong diffuseness instead of distinct reflections from the *F*2 layer; therefore, $foF2$ is not determined on the ionogram. Finally, let us consider the disturbed day of December 22 with $\Sigma Kp = 20+$. This day is less disturbed than the first two days. However, it also has all the signs of a disturbed ionosphere. First of all, there are appreciably more occurrences of sporadic *Es* for December 22 compared to December 23. The day under consideration is characterized by the presence of diffuseness in the *F*2 and *Es* layers. Lateral reflections are present. The number of hops at midday increases to three like on the previous day. The blocking effect is present. However, *M*-modes are absent on this day.

To sum up, the winter storm of December 22−20 shows no fundamental differences in the values of ionospheric parameters during the storm compared to the two previous storms. It is notable that the $foF2$ values are different for spring, summer, and winter. Thus, the mean $foF2$ value at the station of Athens for midday hours of the quiet days is $foF2 = 11.5$ MHz for spring, $foF2 = 9$ MHz for summer, and $foF2 = 7.2$ MHz for winter.

CONCLUSIONS

The analysis performed in this work shows that there are a wide range of changes in ionospheric parameters in the low latitudes over the periods of three intense geomagnetic storms (mostly the main phase), which occurred in different seasons of 2015. A common feature of all storms consists in changes in the following ionospheric parameters according to the data from ionosondes: critical frequencies $foF2$ (decrease), foE, and $foEs$ (increase); a higher degree of diffuseness of signals; the occurrence of lateral reflections; an increase in the multihop pattern in VIS; the effect of blocking signal reflections from the *F*2 layer by the *Es* layer; and the occurrence of *M*-type modes. All these changes are absent under quiet conditions. The analysis was based on the data from ionosondes for the low-latitude station of Athens, Greece (38.00° N; 23.50° E), and partially Nicosia, Cyprus (35.03° N; 33.16° E).

The spring magnetic storm of March 17−20 is the most intense with $Dst_{min} = -223$ nT. The maximum of the disturbance shows the following peculiarities compared to the quiet period: the presence of lateral reflections, the increased diffuseness in the *F*2 layer, and the increased number of reflections during VIS in daytime hours compared to nighttime hours. The example of ionogram with these peculiarities is given.

It has been confirmed that disturbance in the low latitudes leads to a decrease in $foF2$ values compared to the quiet period.

The summer magnetic storm of June 22−25 belongs to the class of intense storms with $Dst_{min} = -204$ nT. The behavior of ionospheric parameters during this storm is characterized by very frequent occurrence of sporadic *Es* layers, *M*-type reflections, and the blocking effect. The example of an ionogram with *M*-type reflections and a multihop pattern via the *Es* layer is given. The fact is extraordinary that there are no lateral reflections during the storm. Like in the previous storm, the $foF2$ values in most cases are lower during this storm compared to the quiet period.

The winter storm of December 20−22 with $Dst_{min} = -155$ nT showed no fundamental differences in abnormal parameters of the ionosphere during the storm compared to the two previous storms. For this storm, the behavior of lateral signals and sporadic *Es* layers was quantitatively estimated by data from the Athens and Nicosia ionosondes ($D = 800$ km). That there is an example of the ionospheric region generating a lateral signal is common for Athens and Nicosia, because the lateral signal is present simultaneously on the ionograms from Athens and Nicosia. Another example shows that the thick *Es* layer stretches along the Earth's surface to a distance of no less than 800 km. The lifetime of this layer is about 7 h.

With respect to seasonal differences, there is a peculiar feature in the storm of March 17−20 (as a season of the equinox): a very low number of occurrences of sporadic *Es* layers. The ionospheric parameters recorded on VIS ionograms for the summer storm of June 22−25 differ from the parameters of the previous storm of March 17−20. For example, lateral signals are absent in summer. It is notable that the $foF2$ values for spring, summer, and winter are different. For example, the mean value of $foF2$ at the Athens station of for midday hours of the quiet days is $foF2 = 11.5$ MHz for spring, $foF2 = 9.0$ MHz for summer, and $foF2 = 7.2$ MHz for winter.

REFERENCES

1. Danilov, A.D., Ionospheric storms in the *F*2-region. Morphology and physics, *Geomagn. Aeron.*, 1985, vol. 23, no. 5, pp. 705−719.

2. Davis, K., *Ionospheric Radio Waves*, Waltham, Mass.: Blaisdell, 1969; Moscow: Mir, 1973.

3. Ban, P.-P., Sun, S.-J., Chen, C., and Zhao, Z.-W., Forecasting of low-latitude storm-time ionospheric *foF*2 using support vector machine, *Radio Sci.*, 2011, vol. 46, RS6008.
https://doi.org/10.1029/2010RS004633

4. Buonsanto, M.J., Ionospheric storms—a review, *Space Sci. Rev.*, 1999, vol. 88, pp. 563−601.

5. Cander, L.R., *Ionospheric Space Weather*, Springer, 2019, ch. 5: Ionospheric Storm Morphology, pp. 95−113.
https://doi.org/10.1007/978-3-319-99331-7_5

6. Cander, L.R. and Mihajlovic, S.J., Forecasting ionospheric structure during the great geomagnetic storms, *J. Geophys. Res.*, 1998, vol. 103, no. A1, pp. 391−398.

7. Goncharenko, L.P., Foster, J., Coster, A., Huang, C., Aponte, N., and Paxton, L., Observations of a positive storm phase on September 10, 2005, *J. Atmos. Sol. Terr. Phys.*, 2007, vol. 69, pp. 1253−1272.

8. Gonzalez, W.D., Joselyn, J.A., Kamide, D., Kroehl, H.W., Rostoker, G., Tsurutani, B.T., and Vasyliunas, P., What is a geomagnetic storm?, *J. Geophys. Res.*, 1994, vol. 99, pp. 5771−5792.

9. Khazanov, G.V., *Kinetic Theory of the Inner Magnetospheric Plasma*, Springer, 2011.

10. Yeh, K.C., Ma, S.Y., Lin, K.H., and Conkright, A., Global ionospheric effects of the October 1989 geomagnetic storm, *J. Geophys. Res.*, 1994, vol. 99, no. A4, pp. 6201−6218.

Translated by E. Makeeva